PNAS RESEARCH ARTICLE | NEUROSCIENCE

Intraneuronal β-amyloid impaired mitochondrial proteostasis through the impact on LONP1

Wenzhang Wang[a,1,2], Xiaopin Ma[a,1], Sabina Bhatta[a], Changjuan Shao[a], Fanpeng Zhao[a], Hisashi Fujioka[b], Sandy Torres[a], Fengqin Wu[a], and Xiongwei Zhu[a,2]

Edited by Lawrence Goldstein, Sanford Consortium for Regenerative Medicine, La Jolla, CA; received October 6, 2023; accepted November 6, 2023

Mitochondrial dysfunction plays a critical role in the pathogenesis of Alzheimer's disease (AD). Mitochondrial proteostasis regulated by chaperones and proteases in each compartment of mitochondria is critical for mitochondrial function, and it is suspected that mitochondrial proteostasis deficits may be involved in mitochondrial dysfunction in AD. In this study, we identified LONP1, an ATP-dependent protease in the matrix, as a top Aβ42 interacting mitochondrial protein through an unbiased screening and found significantly decreased LONP1 expression and extensive mitochondrial proteostasis deficits in AD experimental models both in vitro and in vivo, as well as in the brain of AD patients. Impaired METTL3-m^{6}A signaling contributed at least in part to Aβ42-induced LONP1 reduction. Moreover, Aβ42 interaction with LONP1 impaired the assembly and protease activity of LONP1 both in vitro and in vivo. Importantly, LONP1 knockdown caused mitochondrial proteostasis deficits and dysfunction in neurons, while restored expression of LONP1 in neurons expressing intracellular Aβ and in the brain of CRND8 APP transgenic mice rescued Aβ-induced mitochondrial deficits and cognitive deficits. These results demonstrated a critical role of LONP1 in disturbed mitochondrial proteostasis and mitochondrial dysfunction in AD and revealed a mechanism underlying intracellular Aβ42-induced mitochondrial toxicity through its impact on LONP1 and mitochondrial proteostasis.

Alzheimer's disease | mitochondrial dysfunction | protein aggregate | LONP1 | Aβ42

Significance

Mitochondrial dysfunction is a prominent feature of Alzheimer's disease (AD). Mitochondria have a complex quality control mechanism to maintain proper protein homeostasis, also termed proteostasis. One component is LONP1, a protease essential for protein homeostasis in the mitochondrial matrix. In this study, we show that the AD pathological amyloid peptide Aβ42 interacted with and impaired LONP1 protease activity resulting in proteostasis deficits and mitochondrial dysfunction in AD cell and mouse models. Intracellular Aβ42 reduced LONP1 expression via METTL3-mediated RNA m6A modification. Both reduced LONP1 and impaired mitochondrial proteostasis were validated in human AD brains. This study documents LONP1-associated mitochondrial proteostasis deficits in AD and unveils a mechanism underlying intracellular Aβ-induced mitochondrial dysfunction through its impact on LONP1 and mitochondrial proteostasis.

Mitochondria are conserved organelles that perform multiple essential functions in eukaryotic cells, including energy production, calcium buffering, generation of reactive oxygen species, and regulation of cell death (1). Except for 13 proteins encoded with mtDNA involved in oxidative phosphorylation, most mitochondrial proteins are encoded by the nuclear genome and transported to the organelle, which poses great challenges in the folding of mitochondrial proteins (2). Additionally, as mitochondria are metabolic active organelles where more than 90% of reactive oxygen species are produced, mitochondrial proteins constantly face various stresses, including oxidative stress. To maintain mitochondrial protein homeostasis (termed here as mitochondrial proteostasis), mitochondria developed a complex quality control mechanism to monitor and repair mitochondrial protein misfolding and damage (3), which consists of chaperones and ATP-dependent proteases in each compartment of mitochondria (4, 5). For example, the mitochondrial chaperone HSPD1 and the mitochondrial proteases CLPP and LONP1 mainly localize in the mitochondrial matrix; HTRA2 is an ATP-dependent protease in the mitochondrial intermembrane space, and two complexes of ATP-dependent proteases, i-AAA and m-AAA, localize in the inner membrane of mitochondria. Defects in these proteins cause the accumulation of protein aggregates in mitochondria and mitochondrial dysfunction (6–9). Importantly, genetic mutations in mitochondrial chaperones and proteases cause human diseases with severe neurological symptoms (10–15). For example, CLPP mutations cause autosomal recessive Perrault syndrome with sensorineural hearing loss (11), and LONP1 mutations are associated with cerebral, ocular, dental, auricular, and skeletal syndrome that affects neurological development (12). This underscores the importance of mitochondrial proteostasis regulated by mitochondrial proteases and chaperones in maintaining proper mitochondrial function in the nervous system.

Alzheimer's disease (AD) is the most common neurodegenerative disease in the elderly associated with a decrease in memory and cognitive function. It is characterized by progressive neuronal loss along with hallmark pathologies, including amyloid plaques and neurofibrillary tangles in the hippocampus and cortex. Mitochondrial dysfunction represents an early and prominent feature of AD that likely plays a critical role in the pathogenesis of AD (16, 17). Swollen mitochondria with distorted cristae and related mitochondrial functional deficits have been identified in human AD brains and in transgenic animal models of AD (18–24). Although the mechanisms underlying mitochondrial

The authors declare no competing interest.

This article is a PNAS Direct Submission.

[1]W.W. and X.M. contributed equally to this work.

[2]To whom correspondence may be addressed. Email: wenzhang.wang@case.edu or xiongwei.zhu@case.edu.

This article contains supporting information online at https://www.pnas.org/lookup/suppl/doi:10.1073/pnas.2316823120/-/DCSupplemental.

Published December 13, 2023.

dysfunction in AD have yet to be fully understood, many AD-related pathogenic factors pose increasing challenges to mitochondrial proteostasis. For example, a body of evidence suggests that neuronal toxic amyloid-β (Aβ) peptides translocate into mitochondria (25–27) and alter mitochondrial function (28, 29). Furthermore, oxidative stress, which is one of the pathological features of AD, damages mitochondrial proteins and poses a threat to mitochondrial proteostasis (30). In fact, accumulation of damaged mitochondrial contents, including mtDNA and proteins, has been demonstrated in AD, suggesting that impaired mitochondrial proteostasis may be involved in mitochondrial dysfunction in AD (31, 32).

In the current study, we identified LONP1 as a top Aβ42-interacting mitochondrial protein during an unbiased screening in a cell model expressing intracellular Aβ42 which prompted us to study the potential role of mitochondrial proteostasis in AD. We found significantly reduced LONP1 expression along with increased mitochondrial aggregates in this cell model, which was also replicated in the brain of the CRND8 APP transgenic mouse model in vivo and validated in the brain of human AD patients. In addition to reduced LONP1 expression, the interaction of Aβ42 with LONP1 further reduced the assembly of the LONP1 complex and impaired its protease activity, likely causing LONP1 deficiency in AD. In fact, shRNA-induced LONP1 deficiency in M17 cells caused mitochondrial proteostasis deficits and dysfunction. Importantly, LONP1 overexpression alleviated Aβ-induced deficits in mitochondrial proteostasis and dysfunction both in vitro and in vivo. Collectively, these studies demonstrated a critical role for LONP1 and mitochondrial proteostasis and mitochondrial dysfunction in the pathogenesis of AD.

Results

Aβ42 Interacted with LONP1 in Mitochondria Both In Vitro and In Vivo. It is believed that increased Aβ, especially the more amyloidgenic Aβ42, is involved in the pathogenesis of AD (33). To understand how intracellular Aβ42 disturbs mitochondrial function, we transfected M17 human neuroblastoma cells with a construct of M1-Aβ42 that contained a single open reading frame consisting of the coding sequence of Aβ42 peptide and mitoDsRed connected by the p2a peptide (Fig. 1*A*). The "self-cleavage" of the p2a peptide during translation led to complete separation of the Aβ42 peptide from the mitoDsRed protein as no fusion protein (i.e., Aβ42-mito-DsRed) was found in M1-Aβ42 transfected cells (*SI Appendix*, Fig. S1). Cells transfected with M2-Aβ42 R that expressed the reversed Aβ42 sequence (i.e., Aβ42 R-p2A-mitoDsRed) were used as a control. Western blot analysis confirmed the expression of p2a-DsRed detected by anti-p2a antibody in both M1-Aβ42 and M2-Aβ42 R transfected M17 cells (Fig. 1*A*). Oligomeric Aβ42 species of molecular weight between 15 and 37 kDa were detected by 6E10 antibody only in M1-Aβ42 cells (Fig. 1*A*). Previous studies reported the presence of Aβ in mitochondria that affects mitochondrial function (25–29). Indeed, Aβ42 oligomer was found to be enriched in the mitochondrial fraction in M1-Aβ42 cells (Fig. 1*B*). M1-Aβ42 cells demonstrated mitochondrial fragmentation (Fig. 1 *C* and *D*) and impaired mitochondrial membrane potential (Fig. 1*E*) and mitochondrial ATP levels (Fig. 1*F* and *SI Appendix*, Fig. S2), making it a good model to study the effects of Aβ42 on mitochondria and the underlying mechanisms.

To explore the protein interactome of mitochondria-associated Aβ42, crude mitochondrial fractions of M1-Aβ42 cells were subjected to a coimmunoprecipitation assay with anti-6E10 antibody, and immunoprecipitated proteins were analyzed by mass spectrometry (10.6084/m9.figshare.24262984). The mitochondrial Aβ42 interactome analysis identified mitochondrial proteins in multiple subcompartments of mitochondria that are involved in various mitochondrial functions (Fig. 1*G*). This unbiased screen confirmed the reported interactions between Aβ42 and VDAC1 (34) and mitochondrial respiratory chain complex V (24). Interestingly, LONP1, a mitochondrial AAA+ protease in the matrix, was identified as one of the top-ranked Aβ42-interacting mitochondrial proteins (Fig. 1*H*). Reciprocal co-IP confirmed that anti-6E10 and anti-LONP1 antibodies could pull down LONP1 proteins and Aβ42 oligomers in M1 Aβ42 cells, respectively (Fig. 1*I*). Moreover, Aβ42 oligomers comigrated with the LONP1 complex in blue native (BN) PAGE in the nondenatured state in M1-Aβ42 cells (Fig. 1*J*), and proximity ligation assay with anti-LONP1 and anti-Aβ42 antibodies demonstrated their close association in mitochondria marked by mitoDsRed (Fig. 1*K*), suggesting binding of Aβ42 peptide to LONP1 complexes in mitochondria. To corroborate this finding, we further analyzed the endogenous LONP1-Aβ42 interaction in the brain of 3-mo-old CRND8 APP transgenic mice. In the mitochondrial fraction purified from CRND8 mice brain, LONP1 was coimmunoprecipitated by 6E10 antibody. Multiple immunoreactive bands were also detected by 6E10 antibody in the immunoprecipitants of LONP1-antibody, corresponding to Aβ oligomers of different sizes (Fig. 1*L*).

Aβ42 Impaired Mitochondrial Proteostasis in Neurons. The finding of LONP1-Aβ interaction led us to investigate mitochondrial proteostasis in M1-Aβ42 cells. We first analyzed the expression of mitochondrial chaperone protein and proteases in M1-Aβ42 cells and control M2-Aβ42 R cells. Western blot analysis revealed significantly increased expression of mitochondrial chaperones GRP75 and increased trend of mtUPR transcription factor ATF-5 in M1 Aβ42 cells while the proteasome subunits PSMC5 and PSMD3 were not significantly changed (Fig. 2*A*). Importantly, LONP1 decreased significantly, although no change in CLPP protein, the other protease in the matrix, was found in M1-Aβ42 cells compared to M2-Aβ42 R cells (Fig. 2*A*).

Deficits in mitochondrial matrix proteases cause mitochondrial protein aggregation and induce accumulation of electron-dense aggregates within mitochondria (6). We performed ultrastructure analysis of mitochondria and found that M1-Aβ42 cells showed increased percentage of damaged mitochondria with electron-dense inclusions in the matrix which was rarely seen in the control M2-Aβ42 R cells (Fig. 2*B*). To directly visualize the impact on proteostasis of mitochondrial matrix proteins, M17 cells were cotransfected by M1-Aβ42 and GFP-tagged mitochondrial matrix protein ornithine carbamoyltransferase (OTC-GFP). Fluorescent microscopy analysis revealed large aggregates of GFP-tagged OTC protein in mitoDsRed-labeled mitochondria in M1-Aβ42 cells but not in the control M2-Aβ42 R cells (Fig. 2*C*). Consistently, western blot analysis revealed significantly increased mitochondrial protein in the NP-40 insoluble fraction of purified mitochondria of M1-Aβ42 transfected M17 cells (Fig. 2*D*). Collectively, these data suggest intracellular Aβ42 caused reduced LONP1 expression and mitochondrial proteostasis deficits in neurons.

Impaired Mitochondrial Proteostasis in CRND8 Mice. To explore mitochondrial proteostasis abnormality in AD models in vivo, we analyzed protein levels of mitochondrial proteostasis-related proteins in the brain of CRND8 mice, a widely used APP transgenic mouse model (Fig. 3*A*). No significant change in the expression of these proteins was noted in 3-mo-old CRND8 mice compared with age-matched control mice (Fig. 3*A*). However, western blot analysis revealed significantly reduced expression

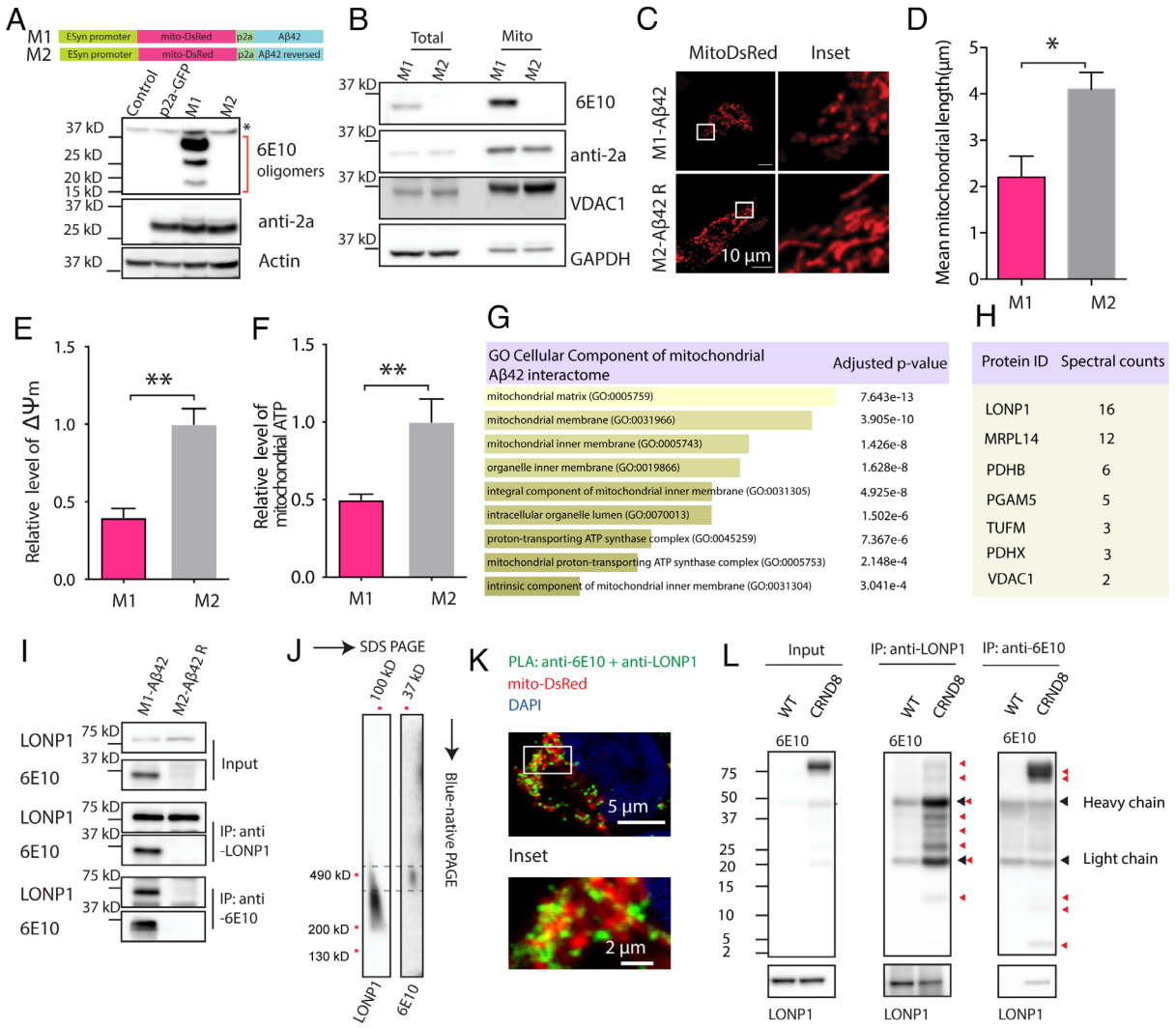

Fig. 1. Mitochondrial Aβ42 interacted with LONP1. (*A*) Diagram of M1 and M2 plasmids and representative western blots showed Aβ expression detected by anti-Aβ42 antibody (6E10, asterisk indicated nonspecific bands) only in M1-Aβ42 transfected M17 cells. Anti-2a detected mitoDsRed-p2a or GFP-p2a in transfected cells. (*B*) Representative western blot confirmed enriched Aβ42 oligomer species in mitochondrial fraction of M1-Aβ42 transfected M17 cells. (*C* and *D*) Representative fluorescence image of mitochondrial labeled by mitoDsRed (*C*) and quantitative analysis of mitochondrial length (*D*) in M1-Aβ42 transfected M17 cells or M2-Aβ42 R transfected control cells. (*E* and *F*) Quantification of mitochondrial membrane potential (*E*) and mitochondrial ATP levels (*F*). (*G* and *H*) Unbiased screen of mitochondrial interactome of Aβ42 with anti-Aβ42 (6E10) antibody in mitochondrial fraction from M1-Aβ42 transfected M17 cells and analysis for the GO cellular component (*G*) and spectral counts of enriched mitochondrial proteins (*H*). (*I*) Representative western blot analysis of Aβ42 and LONP1 expression in immunoprecipitates of anti-Aβ42 (6E10) antibody and anti-LONP1 antibody in M17 cells transfected with M1-Aβ42 and M1-Aβ42 R. (*J*) Representative blue native PAGE demonstrated comigration of Aβ42 oligomer species with mitochondrial protease LONP1 in M17 cells transfected with M1-Aβ42. (*K*) Proximity ligation assay (PLA, green) with antibodies anti-6E10 (Aβ42) and anti-LONP1 in M1 transfected M17 cells. Mitochondria were visualized by transient transfection of mito-DsRed, and the nucleus was stained by DAPI. (*L*) Representative western blot analysis of Aβ42 and LONP1 expression in immunoprecipitates of anti-LONP1 and anti-Aβ42 (6E10) antibody in the brains of wild-type (WT) and CRND8 APP transgenic mice at 3 mo of age. Black arrowheads indicate light and heavy chains, and red arrowheads indicate Aβ42 monomer and oligomers with different molecular weights. Data are means ± SEM from three independent experiments. Student's *t* test, $P^* < 0.05$ and $P^{**} < 0.01$.

of LONP1 along with significantly increased expression of CLPP and GRP75 in 6-mo-old CRND8 mice (Fig. 3*A*). There was a trend toward increased expression of ATF5 in 6-mo-old CRND8 mice although it did not reach statistical significance ($P = 0.19$). Western blot analysis also found significantly increased levels of electron transport proteins in the NP-40 insoluble fractions of purified mitochondria prepared from CRND8 brain homogenates (Fig. 3*B*). Consistently, ultrastructure analysis revealed accumulation of electron-dense aggregates in the matrix of mitochondria (Fig. 3 *C* and *D*), along with increased number of fragmented mitochondria (Fig. 3*E*) in the pyramidal neurons in the hippocampus of 6-mo-old CRND8 mice. Mitochondrial respiration of purified synaptosomal mitochondria from 6-mo-old CNRD8 mice was also impaired (Fig. 3*F*).

Impaired Mitochondrial Proteostasis in the Brains of AD Patients. Next, we investigated mitochondrial proteostasis changes in the hippocampal tissues from AD and age-matched control patients. There was significantly decreased expression of LONP1 and CLPP in the hippocampus from AD patients compared with age-matched controls (*SI Appendix*, Fig. S3*A*). ATF5 expression was increased while no significant changes of AFG3L2, YME1L1, HTRA2, GRP75, and HSPD1 were noted (*SI Appendix*, Fig. S3*A*). Significantly increased levels of electron transport proteins were found in the NP-40 insoluble fractions of purified mitochondria prepared from human cortical brain tissues of AD cases (*SI Appendix*, Fig. S3*B*). Electron microscopy analysis of mitochondria using a series of electron micrographs taken from biopsied human brain tissues often identified

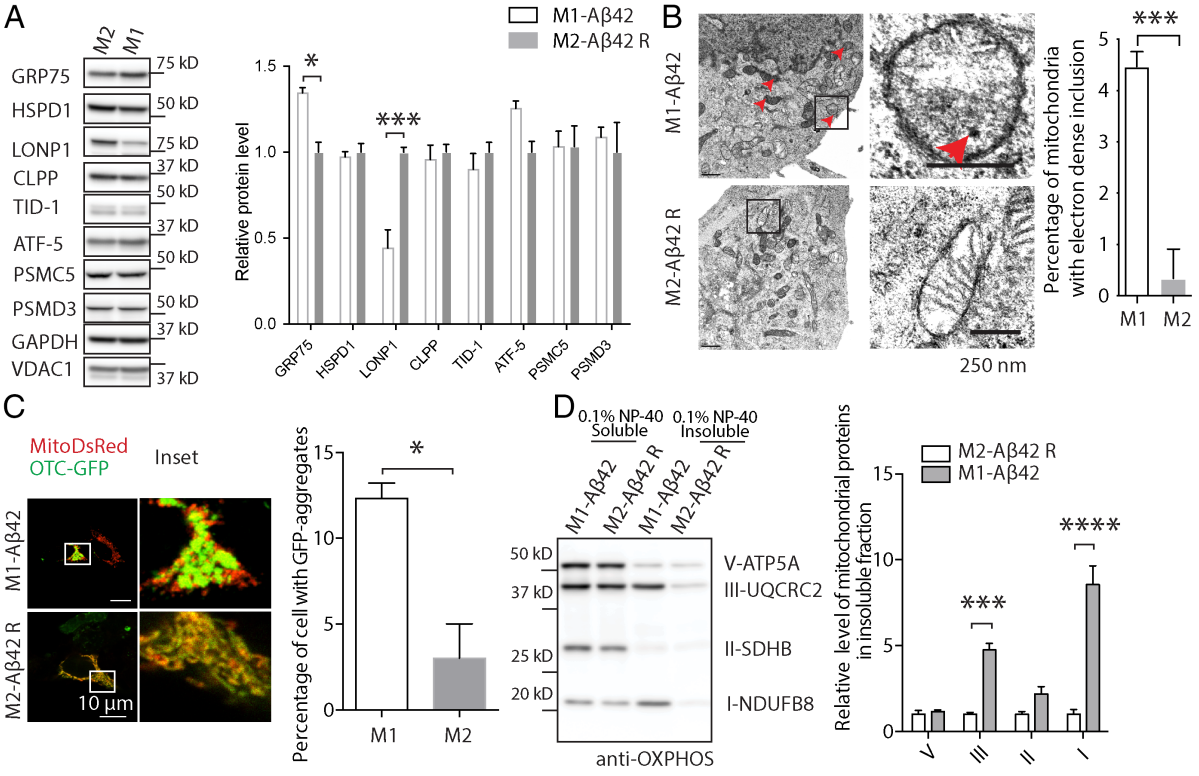

Fig. 2. Intracellular Aβ42 caused mitochondrial proteostasis defects in M17 cells. (*A*) Representative western blot and quantitative analysis of mitochondrial proteostasis–related proteins in M1-Aβ42 transfected M17 cells or M2-Aβ42 R transfected control cells. (*B*) Representative electron micrograph and quantitative analysis of electron-dense inclusions in the mitochondria of M1-Aβ42 transfected M17 cells or M2-Aβ42 R transfected control cells. (*C*) Representative fluorescence image and quantitative analysis of OTC-GFP aggregates in the mitochondria labeled by mitoDsRed in M1-Aβ42 transfected M17 cells. (*D*) Representative western blot and quantitative analysis of mitochondrial ETC proteins in the 0.1% NP40-insoluble mitochondrial fraction from M1-Aβ42 transfected M17 cells or M2-Aβ42 R transfected control cells. Data are means ± S.E.M from three independent experiments. Two-way ANOVA followed by Bonferroni correction and Student's *t* test, $P^{*} < 0.05$, $P^{***} < 0.001$, and $P^{****} < 0.0001$.

electron-dense inclusions within mitochondria in the pyramidal neurons in the cortex from AD patients which were rarely seen in age-matched controls (*SI Appendix*, Fig. S3*C*). Collectively, these data demonstrated reduced LONP1 and increased mitochondrial protein aggregates in the AD brain which suggests impaired mitochondrial proteostasis in AD.

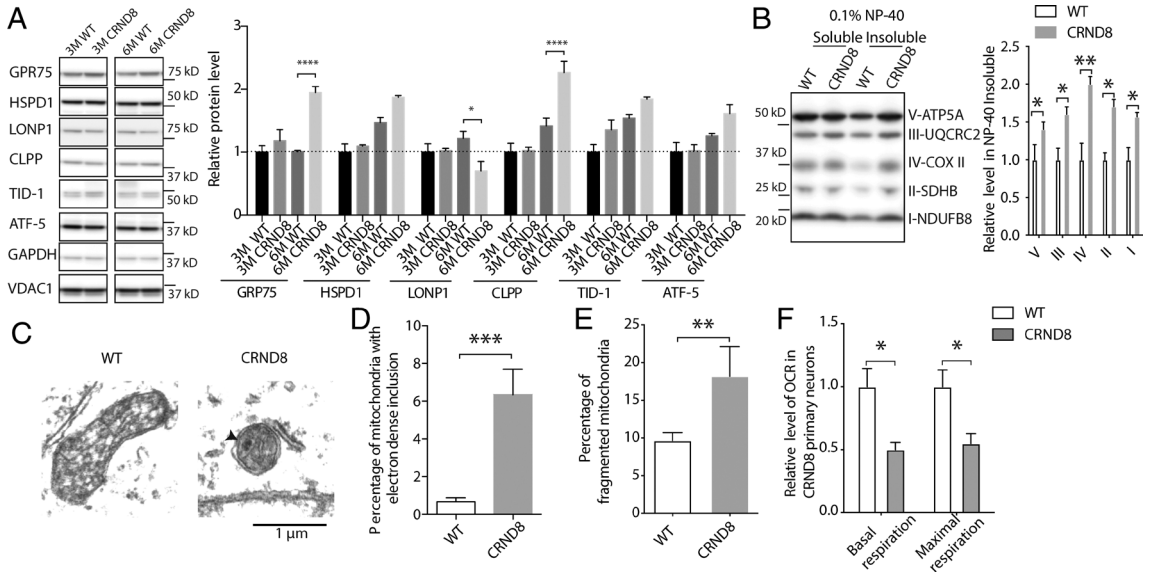

Fig. 3. Impaired mitochondrial proteostasis in CRND8 APP transgenic mice. (*A*) Representative western blot and quantitative analysis of mitochondrial proteostasis–related proteins in the brains of 3 mo and 6-mo-old wild-type (WT) and CRND8 APP transgenic mice ($n = 3$ mice in each group). (*B*) Representative western blot and quantitative analysis of mitochondrial ETC proteins in the 0.1% NP40-insoluble mitochondrial fraction of cortical lysates from 6-mo-old WT and CRND8 animals. (*C* and *D*) Representative electron micrograph (*C*) and quantitative analysis of mitochondrial electron-dense inclusion (*D*) and fragmented mitochondria (*E*) in the hippocampal pyramidal neurons of 6 mo WT and CRND8 animals (Scale bar, 1 μm). (*F*) Mitochondrial respiration assay of synaptosomal mitochondria of 6 mo WT and CRND8 mice. Data are means ± SEM from three independent experiments. Two-way ANOVA followed by Bonferroni correction and Student's *t* test, $P^{*} < 0.05$, $P^{***} < 0.001$, and $P^{****} < 0.0001$.

Reduced LONP1 mRNAs in AD Models Associated with METTL3-m^{6}A Dysregulation. To explore the possible mechanism(s) underlying LONP1 reduction in AD, we further investigated the LONP1 expression at mRNA levels and found that the LONP1 mRNA level was also decreased in M1-Aβ42 cells (Fig. 4*A*), in CRND8 mouse brains at 3 mo of age (Fig. 4*B*) as well as in the human AD cortical tissues (Fig. 4*C*) though there were no changes of mRNA levels of actin or β-tubulin (*SI Appendix*, Fig. S4). N6-methyladenosine (m^{6}A) modification of RNA affected the stability of RNA transcripts (35). We recently found significantly reduced RNA m^{6}A deposit along with reduced expression of m^{6}A writer METTL3 in AD neurons (36). In silico analysis of m^{6}A modification identified several m^{6}A sites in the open reading frame of human and rodent LONP1 mRNA transcripts (Fig. 4*D*). Indeed, LONP1 mRNA levels and protein levels were significantly reduced in primary rat cortical neurons at DIV10 with METTL3 knockdown by AAV transduction at DIV7 (Fig. 4 *E* and *F*), suggesting LONP1 mRNA expression could be impacted by m^{6}A modification. Consistently, M1-Aβ42 cells showed a significant reduction in m^{6}A RNA level by dot blot analysis of cellular RNA (Fig. 4*G*). RT-PCR after m^{6}A RNA-IP further revealed significantly reduced m^{6}A deposition in LONP1 in M1-Aβ42 cells, which was rescued by overexpression of METTL3 (Fig. 4*H*). Furthermore, overexpressed METTL3 in M1 cells significantly slowed down the RNA decay of LONP1 mRNA but not METTL3-m^{6}A independent RNA transcripts such as 18 s rRNA and GAPDH mRNA (Fig. 4*I*), suggesting that METTL3-m^{6}A dysregulation likely mediated intracellular Aβ-induced LONP1 mRNA reduction which resulted in reduced LONP1 expression in AD.

Aβ42 Impaired LONP1 Complex Assembly and Function. Given the interaction between LONP1-Aβ42, we suspect that intracellular Aβ42 may directly impact the function of LONP1 in addition to its effect on reduced LONP1 expression. To determine whether Aβ binding affects protease activity of LONP1, we incubated recombinant LONP1 protein with either synthetic Aβ42 peptide or scrambled Aβ42 control peptide followed by the addition of LONP1 fluorogenic substrate FITC-casein in ATP buffer to measure ATP-dependent protease activity of LONP1 (Fig. 5*A*). We found that Aβ42 peptides significantly inhibited the release of fluorescent FITC tag from casein in a dose- and time-dependent manner (Fig. 5*A*), suggesting impaired protease activity of LONP1 proteins by Aβ42. High-molecular-weight LONP1 complex is the

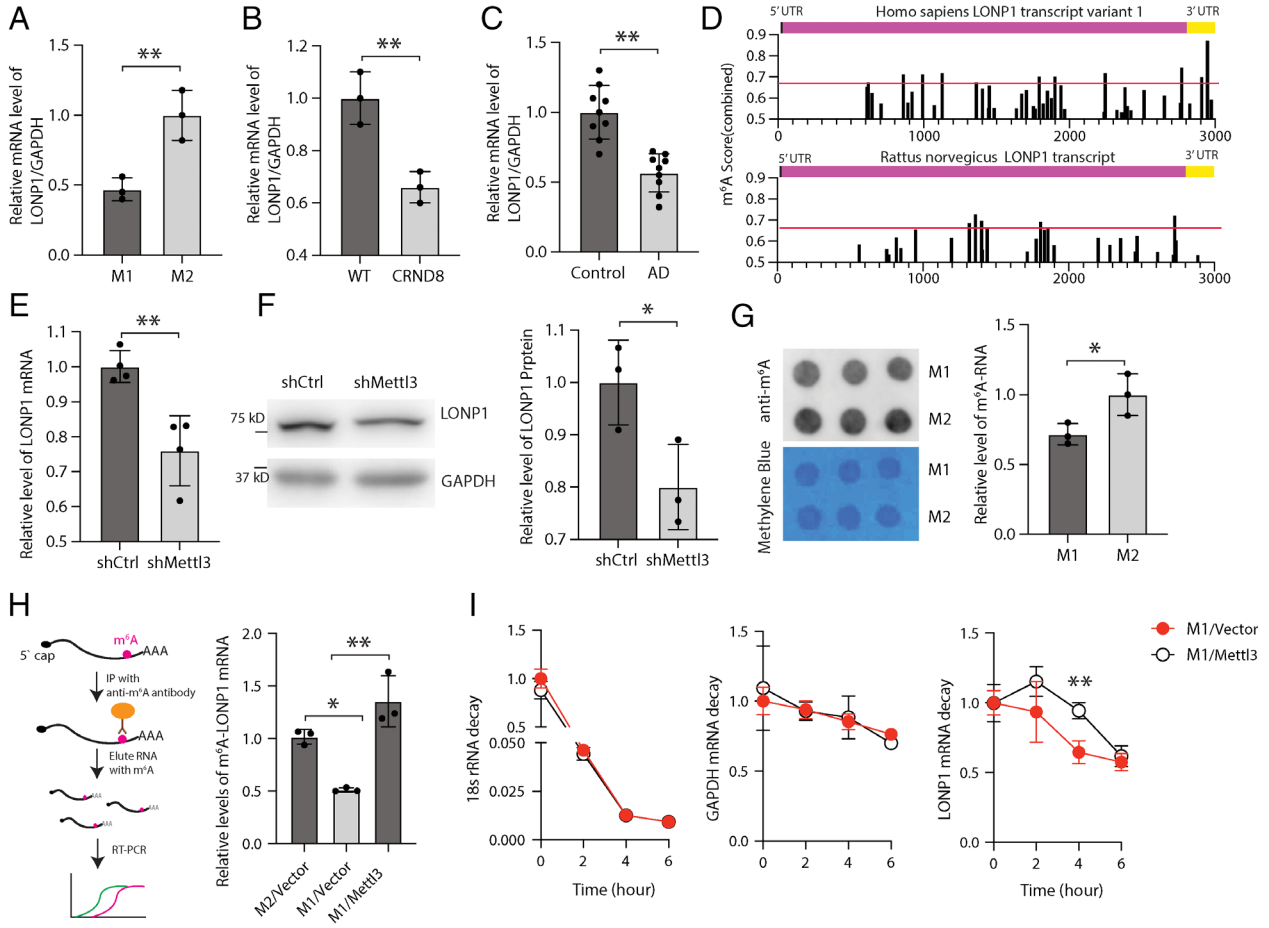

Fig. 4. LONP1 transcript is regulated by METTL3-mediated m^{6}A modification. (*A* and *B*) Real-time PCR analysis of LONP1 gene expression adjusted by GAPDH mRNA in M1-M17 cells (*A*), CRND8 cortical tissues (*B*), and human brain cortical tissues (*C*). (*D*) The potential m^{6}A methylation sites of human and rat LONP1 mRNA by a sequence-based N6-methyladenosine (m^{6}A) modification site predictor (SRAMPA, http://www.cuilab.cn/sramp/). Red lines indicate the threshold of the m6A sites with very high confidence. (*E* and *F*) Primary rat cortical neurons from E16–18 embryos were infected with AAV-GFP-shMettl3 or AAV-GFP-shCtrl on ~DIV 7. Primary neurons were extracted at DIV15 for real-time qPCR analysis (*E*) and immunoblot analysis (*F*) of LONP1 expression. (*G*) Dot-blot analysis of m^{6}A modification of cellular RNA extracted from M1 and M2 transfected M17 cells. Methylene blue stain indicated an equal loading of RNA samples. (*H*) Anti-m6A immunoprecipitation of RNA extracted from M17 cells followed by RT-PCR with specific primers to amplify LONP1 mRNA with m6A modification. (*I*) RNA decay assay of LONP1 mRNA, 18 s rRNA, and GAPDH mRNA in M1-transfected M17 cells with or without METTL3 overexpression treated with actinomycin D (5 μg/mL) for indicated times. Data are means ± SEM from three independent experiments. One-way ANOVA followed by Bonferroni correction and Student's *t* test, n.s., nonsignificant, $P^* < 0.05$, and $P^{**} < 0.01$.

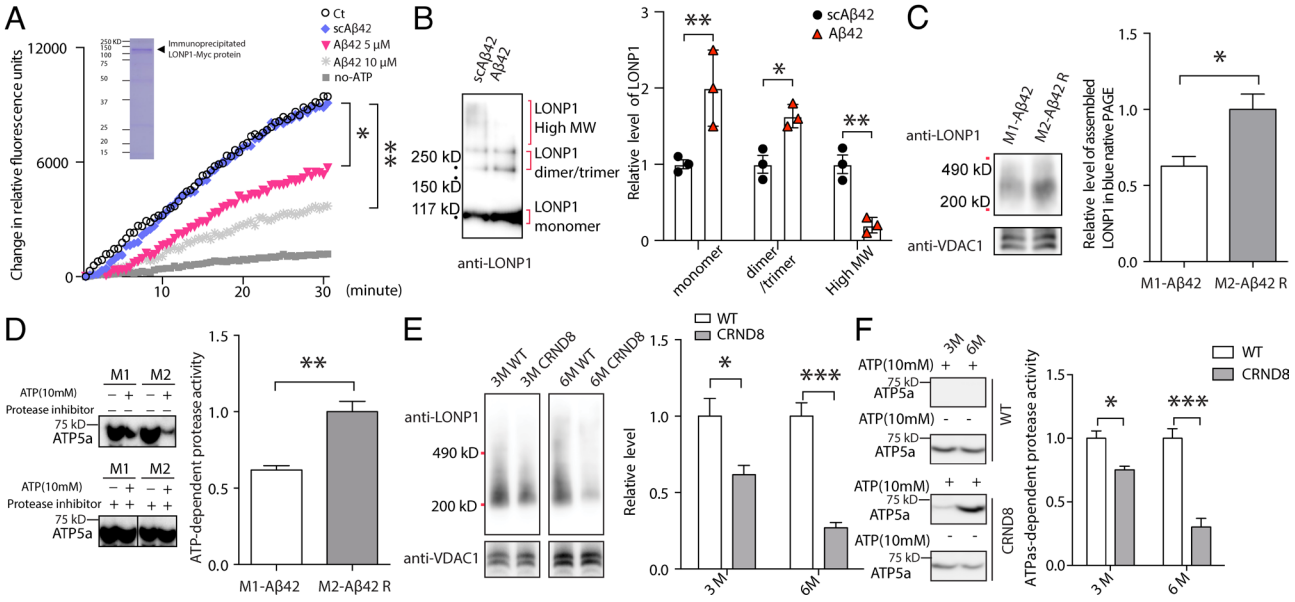

Fig. 5. Aβ42 impaired LONP1 complex assembly and protease activity. (*A*) ATP-dependent protease activity of recombinant LONP1-myc proteins was inhibited by preincubation with synthetic Aβ42 peptides but not Aβ42 scramble control peptides (scAβ42) in vitro. (*B*) Representative western blot and quantitative analysis of cross-linked LONP1-myc proteins incubated with synthetic Aβ42 peptides. (*C*) Blue native PAGE and quantitative analysis of the LONP1 complex in mitochondrial fraction of M1-Aβ42 and M1-Aβ42 R transfected M17 cells. (*D*) Representative western blot and quantitative analysis of ATP5a substrate after mitochondrial protease activity assay in the absence and presence of protease inhibitors using mitochondria purified from M1-Aβ42 and M1-Aβ42 R transfected M17 cells. (*E*) Representative blue native PAGE and quantitative analysis of the LONP1 complex in purified brain mitochondria from wild-type (WT) and CRND8 mice. (*F*) Representative western blot and quantitative analysis of substrate ATP5a after mitochondrial protease activity assay in the absence and presence of ATP using mitochondria purified from the brain of 3- and 6-mo-old CRND8 APP transgenic mice. Data are means ± SEM from three independent experiments. Two-way ANOVA followed by Bonferroni correction for multiple comparisons and Student's *t* test, $P^* < 0.05$, $P^{**} < 0.01$, and $P^{***} < 0.001$.

functional form of this AAA+ protease in the mitochondrial matrix (37). Aβ42 caused decreased levels of high molecular weight LONP1 complexes and increased levels of LONP1 monomers and dimer/trimers, suggesting that Aβ42 peptides impaired assembly of recombinant LONP1 proteins (Fig. 5*B*). Indeed, BN-PAGE revealed significantly decreased levels of functional LONP1 complexes in M1-Aβ42 cells (Fig. 5*C*). Consistently, ATP-dependent protease activity in the mitochondrial fraction of M1-Aβ42 M17 cells was significantly lower than that in the control M2-Aβ42 R M17 cells (Fig. 5*D*). Moreover, levels of LONP1 complexes (Fig. 5*E*) and ATP-dependent protease activity (Fig. 5*F*) in the mitochondrial fraction were also significantly reduced in the brain of 3-mo-old CRND8 mice, and further reduced in the brain of 6-mo-old CRND8 mice in vivo when compared to age-matched WT mice. These findings suggest that intracellular Aβ42 likely caused significant LONP1 deficiency through both the impairment of its assembly and protease activity and modulation of its expression.

LONP1 Knockdown Impaired Mitochondrial Proteostasis and Function in Neurons. To determine whether LONP1 deficiency affected mitochondria proteostasis and function in neurons, we down-regulated LONP1 expression in M17 cells by LONP1 shRNA (*SI Appendix*, Fig. S5*A*). LONP1 knockdown in M17 cells resulted in significantly increased expression of GRP75 and CLPP and significantly decreased TID-1 (*SI Appendix*, Fig. S5*A*). Furthermore, western blot analysis revealed significantly increased levels of electron transport proteins in the NP-40 insoluble fractions of purified mitochondria in LONP1 shRNA-transfected cells (*SI Appendix*, Fig. S5*B*). Fluorescent microscopy analysis also found accumulation of large aggregates of GFP-tagged OTC protein in mitoDsRed-labeled mitochondria in LONP1 shRNA transfected cells (*SI Appendix*, Fig. S5*C*), suggesting impaired mitochondrial proteostasis in LONP1 shRNA transfected cells. Indeed, significantly greater numbers of damaged mitochondria with electron-dense inclusions were found in LONP1 shRNA transfected cells when compared with control cells (*SI Appendix*, Fig. S5*D*). Importantly, mitochondria became fragmented, and mitochondrial oxygen consumption rate was significantly reduced in LONP1 shRNA transfected cells (*SI Appendix*, Fig. S5 *E* and *F*), suggestive of mitochondrial dysfunction. Taken together, these data demonstrated that reduced LONP1 expression impaired mitochondrial proteostasis and led to mitochondrial fragmentation and dysfunction in neurons.

We also tested knockdown of LONP1 by shRNA in M1-Aβ42 cells. Interestingly, LONP1 knockdown in the M1-Aβ42 cells failed to exaggerate mitochondrial respiration deficits measured by basal or maximal OCR (*SI Appendix*, Fig. S5*G*) or percentage of damaged mitochondria with electron-dense inclusions (*SI Appendix*, Fig. S5*H*) in EM analysis as compared to control shRNA-transfected M1-Aβ42 cells, suggesting that intracellular Aβ42 peptide likely causes mitochondrial deficits through a LONP1-dependent mechanism.

LONP1 Rescued Aβ42-induced Mitochondrial Proteostasis Deficits In Vitro. To determine whether LONP1 deficiency mediates impaired mitochondrial proteostasis in the AD model, we investigated whether overexpression of LONP1 could rescue mitochondrial deficits. Indeed, coexpression of LONP1 in M1-Aβ42 M17 cells restored GRP75 and ATF5 expression to the level comparable to control cells (Fig. 6*A*). Western blot analysis of the NP-40 insoluble fractions of purified mitochondria revealed decreased electron transport chain (ETC) proteins after LONP1 expression in M1-Aβ42 M17 cells, suggesting improved solubility of ETC proteins by LONP1 expression (Fig. 6*B*). Aβ-induced accumulation of large aggregates of GFP-tagged OTC protein in mitoDsRed-labeled mitochondria was also rescued by LONP1 overexpression (Fig. 6*C*), suggesting the restoration of mitochondrial proteostasis. As a result, LONP1 overexpression led to alleviation

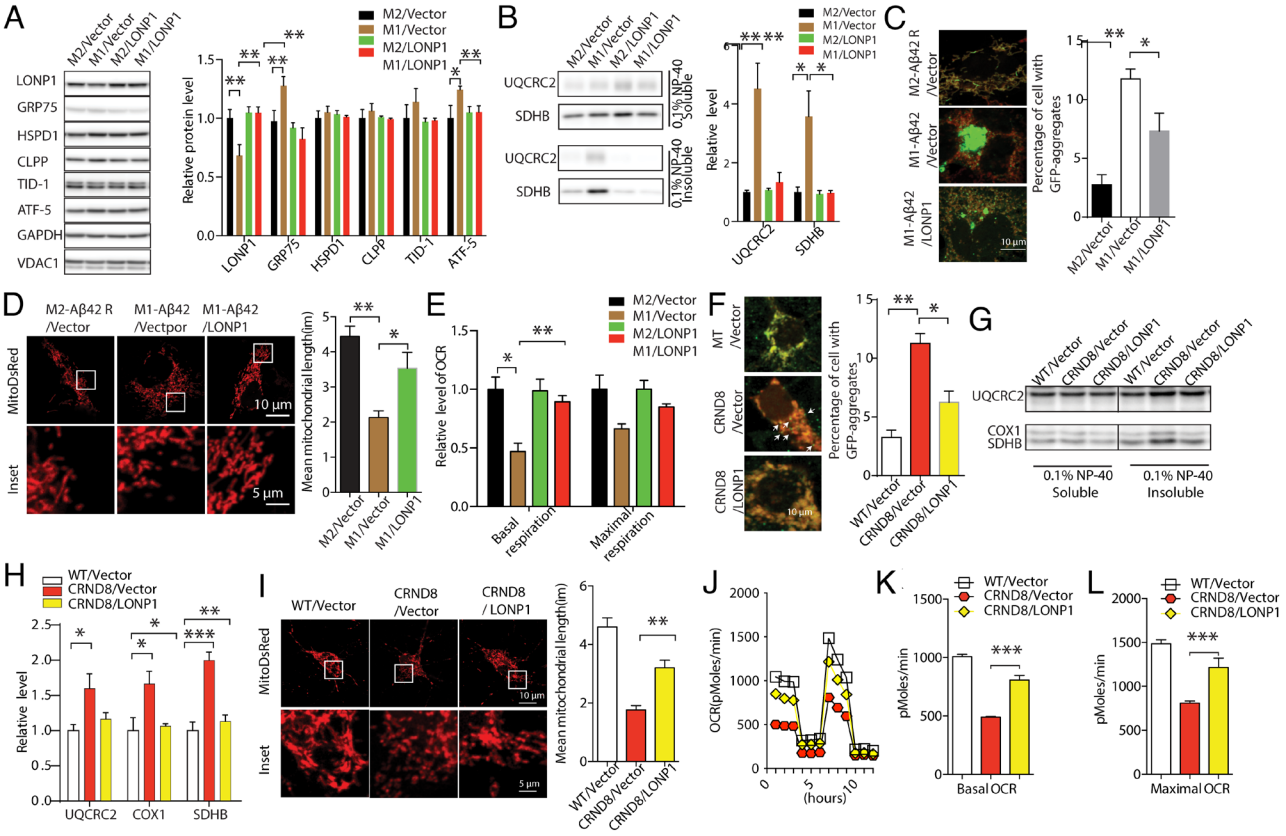

Fig. 6. LONP1 rescued Aβ42-induced mitochondrial proteostasis defects and mitochondrial dysfunction in vitro. (*A*) Representative western blot and quantitative analysis of mitochondrial proteostasis–related proteins demonstrated that overexpression of LONP1 ameliorated intracellular Aβ42-induced mitochondrial unfold protein response in M17 cells. (*B*) Representative western blot and quantitative analysis of mitochondrial ETC proteins in the 0.1% NP40-insoluble mitochondrial fraction demonstrated that overexpression of LONP1 ameliorated intracellular Aβ42-induced mitochondrial protein aggregates in M17 cells. (*C–E*) LONP1 overexpression rescued intracellular Aβ42-induced GFP-OTC aggregates in the mitochondrial matrix (*C*), mitochondrial fragmentation (*D*), and oxygen consumption rate (*E*) in M17 cells. (*F*) LONP1 overexpression rescued GFP-OTC aggregates in the mitochondrial matrix in primary cortical neurons of CRND8 at days in vitro (DIV) 14. (*G* and *H*) Representative western blot and quantitative analysis of mitochondrial ETC proteins in the 0.1% NP40-insoluble mitochondrial fraction of CRND8 primary cortical neurons transduced by lenti-LONP1 virus. (*I*) LONP1 overexpression rescued mitochondrial fragmentation in primary cortical neurons of CRND8. (*J–L*) Quantification of basal respiration (*K*) and maximal respiration (*L*) in wild-type (WT) CRND8 neurons transduced by lenti-LONP1 virus. Data are means ± SEM from three independent experiments. One-way ANOVA followed by Bonferroni correction, $P^{*} < 0.05$, $P^{**} < 0.01$, $P^{***} < 0.001$, and $P^{****} < 0.0001$.

of mitochondrial morphology (Fig. 6*D*) and respiratory function deficits (Fig. 6*E*) in M1-Aβ42 transfected cells.

We previously reported mitochondrial morphological and functional deficits in primary cortical neurons from CRND8 APP transgenic mice (38). To corroborate our findings in primary neurons, we transfected primary cortical neurons isolated from CRND8 mice with lenti-LONP1 virus at DIV 7 and analyzed at DIV14. CRND8 neurons demonstrated increased large aggregates of GFP-tagged OTC protein in mitoDsRed-labeled mitochondria which was alleviated by the expression of LONP1 (Fig. 6*F*). Similarly, LONP1 expression also reduced ETC protein deposit in the NP-40 insoluble fractions of purified mitochondria from CRND8 neurons (Fig. 6 *G* and *H*). Furthermore, LONP1 expression significantly ameliorated mitochondrial fragmentation (Fig. 6*I*) and restored basal OCR in CRND8 neurons compared with CRND8 neurons transfected with control virus containing empty-vector (Fig. 6 *J–L*)

LONP1 Expression Rescued Mitochondrial and Cognitive Defects in CRND8 Mice. To determine whether LONP1 expression could rescue mitochondrial dysfunction and AD-related deficits in vivo, we injected the lentivirus vectors expressing LONP1 protein into the CA1 region of both hemispheres of 3-mo-old CRND8 mice. Three months after virus injection, the mice were analyzed. The increased expression of the LONP1 protein in the hippocampus of CRND8 mice was confirmed by immunostaining with anti-myc antibody and western blot analysis of isolated hippocampus tissues (Fig. 7*A*). Imaging and quantification analysis revealed that fragmented and often round-shaped mitochondria in CRND8 pyramidal neurons were rescued by LONP1 expression (Fig. 7 *B–D*).

These age- and gender-matched mice were subjected to cognitive tests before killing. In the contextual fear conditioning test, CRND8 mice demonstrated significantly lower freezing time which was rescued by the LONP1 expression (Fig. 7*E*). Similarly, the impaired spatial working memory of CRND8 mice, analyzed by Y-maze test, was also restored by LONP1 expression (Fig. 7*F*), suggesting LONP1 expression rescued cognitive deficits in CRND8 mice. Despite that a gender difference was reported in mitochondrial function and mitophagy after exogenous stress (39–41), no gender-specific effects were noted in our study. Consistent with improved cognitive function, immunocytochemical analysis of synaptophysin revealed that decreased levels of synaptophysin in the hippocampus of CRND8 mice were also rescued by LONP1 overexpression (Fig. 7*G*).

Discussion

In this study, we established a neuronal cell model to study the effects of intracellular Aβ42 on mitochondria. Through an unbiased

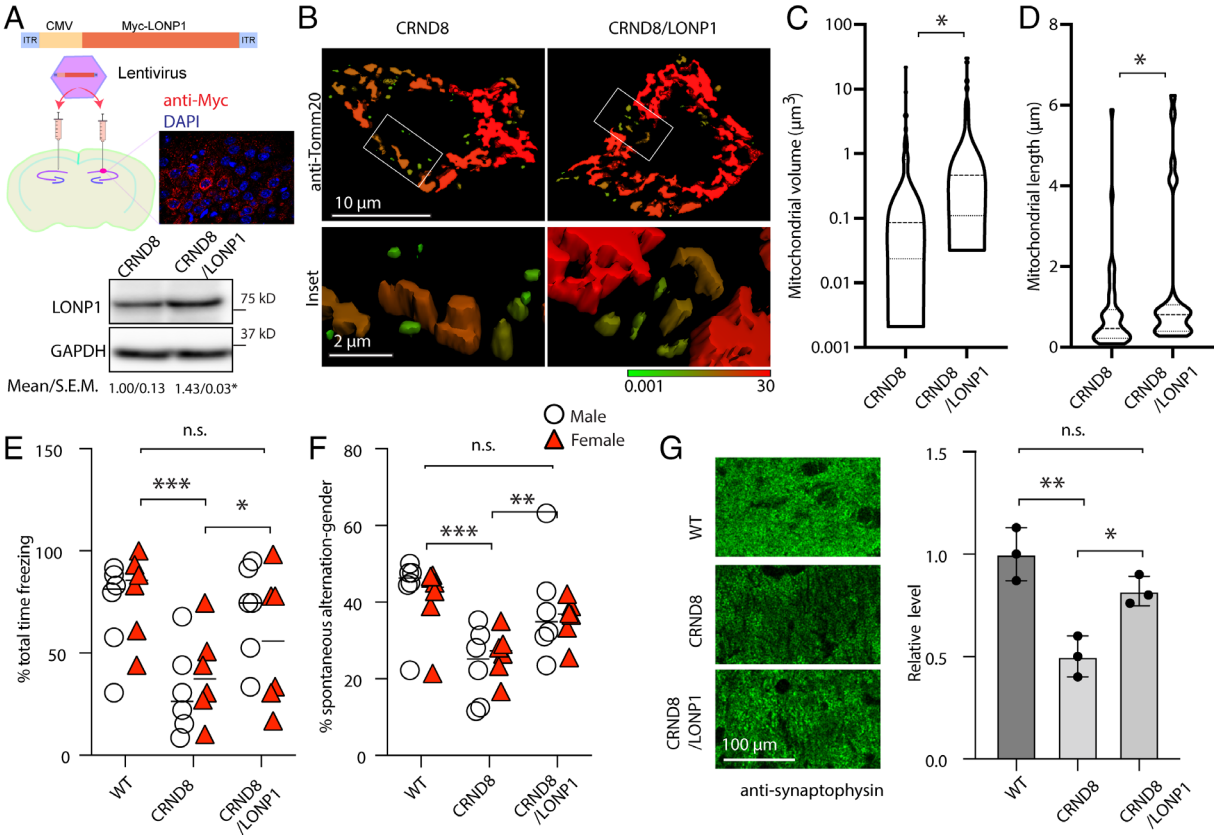

Fig. 7. LONP1 expression rescued mitochondrial and cognitive deficits in CRND8 APP transgenic mice. (*A*) Diagram of lentivirus vector encoding myc-LONP1 injected into the CA1 area of the mouse brain and the representative immune-fluorescent image confirmed expression of myc-LONP1 in the hippocampus. Immunostaining with anti-myc antibody and western blot analysis of isolated hippocampal tissues confirmed the expression of LONP1 after virus injection. (*B*) Neuronal mitochondria in the CA1 regions were analyzed by 3D visualization of anti-Tomm20 confocal images. Green to red color denoted the 3D volume of mitochondria from min to max. (*C* and *D*) Quantification of the volume (*C*) and length (*D*) of neuronal mitochondria in the CA1 regions in 6-mo-old CRND8 mice with or without LONP1 virus injection at 3-mo-old. (*E*) The quantification of % of total freezing time of age- and gender-matched wild-type (WT, $n = 13$) or CRND8 mice with ($n = 12$) or without LONP1 ($n = 12$) virus injection in the contextual fear condition test. (*F*) The quantification of % of spontaneous alternation of WT or CRND8 mice with or without LONP1 virus injection in the spatial Y-maze test. (*G*) Representative immunostaining and quantitative analysis of synaptophysin in the CA1 regions of WT or CRND8 mice with or without LONP1 virus injection. Data are means ± SEM from three independent experiments. One-way ANOVA followed by Bonferroni correction and Student's *t* test, n.s., nonsignificant, $P^* < 0.05$, $P^{**} < 0.01$, and $P^{***} < 0.001$.

screening, LONP1 was identified as one of the top Aβ42-interacting mitochondrial proteins. Interestingly, we found significantly decreased LONP1 expression/activity and extensive mitochondrial proteostasis deficits such as increased insoluble ETC protein aggregates in the matrix along with mitochondrial fragmentation and impaired mitochondrial respiration in this cell model of AD. Similar LONP1 reduction and mitochondrial proteostasis deficits were also found in the brain of CRND8 mice in vivo and validated in the brain of human AD patients. Furthermore, Aβ42 was found enriched in mitochondria and interacted with LONP1 which impaired LONP1 assembly and protease activity both in vitro and in vivo. Importantly, LONP1 knockdown caused mitochondrial proteostasis deficits and dysfunction while restored expression of LONP1 in vitro and in the brain of CRND8 APP transgenic mice rescued Aβ-induced mitochondrial deficits and cognitive deficits. These results demonstrated a critical role of LONP1 in the disturbed mitochondrial proteostasis and mitochondrial dysfunction in AD and revealed a mechanism underlying intracellular Aβ42-induced mitochondrial toxicity through the impact on LONP1.

Multiple lines of evidence demonstrated accumulation of damaged mitochondria in the AD brain associated with compromised mitophagy, and enhanced mitophagy alleviated mitochondrial and neuronal deficits in AD models (42–44). At the suborganelle level, alterations in mitochondrial proteostasis were also associated with neurodegenerative diseases and aging (45), yet not much study was done in AD. Prior studies demonstrated accumulation of oxidative damaged mitochondrial proteins and an activation of mitochondrial unfolded protein response (mtUPR) in AD models and in AD patient brains which suggests the potential involvement of impaired mitochondrial proteostasis (46, 47). Consistently, we found increased GRP75, a mitochondrial heat shock protein involved in the proper folding of newly imported protein (48), and ATF-5, a specific mtUPR transcription factor in mammals (49), in our models which confirmed an activation of mtUPR response. More importantly, we found cardinal features of disturbed mitochondrial proteostasis such as increased ETC protein aggregates in the NP-40 insoluble fractions and remarkable protein aggregates in the mitochondrial matrix revealed by both immunofluorescent microscopy and transmission electron microscopy investigations in AD models as well as in the brain of AD patients. These data not only provided strong evidence supporting the notion of a disturbed mitochondrial proteostasis in AD but also suggested that the mitochondrial matrix is a focal point of mitochondrial proteostasis deficits in AD.

As one of the most protein-concentrated environment in the cell (50), the mitochondrial matrix maintains its proteostasis through a set of chaperones and proteases. Interestingly, intracellular Aβ expression caused selective reduction of LONP1, a key AAA+ protease in the matrix, and Aβ also inhibited LONP1 protease activity. Similarly reduced expression of LONP1 was also

found in the brain of CRND8 mice and human AD patients. Impaired LONP1 activity was even found in 3-mo-old CRND8 mice before significant amyloid pathology began to develop, suggesting LONP1 reduction and dysfunction is an early feature during the disease and may be involved in the mitochondrial proteostasis deficits in AD. In this regard, LONP1 knockdown in neurons caused activation of mtUPR and increased insoluble ETC protein aggregates in the matrix along with mitochondrial fragmentation and impaired mitochondrial respiration which were very similar to the mitochondrial proteostasis deficits and dysfunction observed in the AD brain and AD models. It was of interest to note that LONP1 knockdown did not exacerbate mitochondrial deficits in the AD cell model expressing intracellular Aβ, suggesting that Aβ induced mitochondrial proteostasis deficits and dysfunction through the same pathway as LONP1 deficiency. Indeed, overexpression of LONP1 rescued mitochondrial proteostasis deficits and alleviated mitochondrial function and cognitive deficits both in vitro and in vivo. These data thus established a critical role of LONP1 deficiency in mediating Aβ42-induced mitochondrial proteostasis deficits in AD.

How does Aβ impair LONP1 function? It appears that multiple mechanisms are likely involved. First, intracellular Aβ caused reduced LONP1 expression. Real-time PCR demonstrated reduced LONP1 mRNA in neuronal cells expressing intracellular Aβ suggesting that Aβ regulated LONP1 expression at the transcriptional level. The possibility that posttranscriptional level regulation is also involved in the regulation of LONP1 expression cannot be ruled out. In this regard, it is known that mRNA stability could be affected by m^6A modification and we recently reported significantly reduced METTL3-m^6A signaling in AD neurons (36). In fact, our in silico study found that LONP1 mRNA contains m^6A modification sites and METTL3 knockdown caused significantly reduced mRNA and protein expression of LONP1 in neurons. Indeed, intracellular Aβ caused significantly reduced m^6A modification of LONP1 mRNA which was rescued by METTL3 overexpression. Rescued m^6A modification slowed down the decay of LONP1 mRNA. Therefore, Aβ likely caused reduced LONP1 expression at least in part through impaired METTL3-m^6A signaling in neurons. It should be mentioned that enhanced LONP1 protein expression was found in SHSY5Y cells treated by extraneuronal Aβ25–35 peptide (51). The discrepancy may be due to the use of different Aβ species or how they were applied since extracellularly applied Aβ was shown to block mitochondrial import of nuclear-encoded mitochondrial proteins (52) which may induce different mitochondrial responses than intracellular Aβ. Second, Aβ inhibited LONP1 activity in a time- and dose-dependent manner in vitro, and reduced mitochondrial ATP-dependent protease activity was also found in the AD cell model and CRND8 brain. Consistent with the mitochondrial matrix localization of Aβ, LONP1 in the matrix was identified as a protein interacted with Aβ through an unbiased mass spectrometry screen, and Aβ-LONP1 interaction was confirmed both in vitro and in vivo, suggesting that Aβ-LONP1 interaction could mediate Aβ-induced LONP1 inhibition. The ATP-dependent protease activity of LONP1 is dependent on its proper assembly into a homohexameric ring-shaped complex (49). Mutations in LONP1 that affect its ability to form complex cause defects in ATP-dependent proteolysis and mitochondrial proteostasis (12). Indeed, Aβ treatment or expression caused significantly reduced functional LONP1 complexes both in vitro and in vivo, suggesting that Aβ-LONP1 interaction mediated Aβ-induced LONP1 inhibition likely by impacting LONP1 assembly. This may be the major mechanism contributing to mitochondrial proteostasis deficits at early stage because the level of functional LONP1 complexes along with mitochondrial ATP-dependent protease activity was reduced in the brain of 3-mo-old CRND8 mice when LONP1 protein expression did not change. Nevertheless, it remains to be determined whether Aβ prevents the functional LONP1 assembly or destabilizes the LONP1 functional complexes. Reduced LONP1 complexes were accompanied by increased LONP1 monomer or dimer/trimers in the cell-free system but not in the AD cell model or the brain of CRND8 mice, suggesting that LONP1 monomers and dimer/trimers may be degraded in cells which could contribute to the decreased proteins levels of LONP1 in our models. It was reported that oxidative modification also causes LONP1 dysfunction (53) and Aβ is known to induce oxidative stress. It would be of interest to investigate whether oxidative modification of LONP1 is also involved in Aβ-induced LONP1 dysfunction.

In summary, we provided evidence demonstrating LONP1-associated mitochondrial proteostasis deficits in AD experimental models and in the brain of AD patients and unveiled a mechanism underlying the intracellular Aβ-induced mitochondrial proteostasis deficits through the impact on LONP1 that is likely playing a critical role in mitochondrial dysfunction in the pathogenesis of AD. Our study suggested that LONP1 dysregulation and mitochondrial proteostasis deficits might provide promising therapeutic targets for future AD treatment.

Materials and Methods

Cell Culture. Human neuroblastoma M17 cells were maintained in OptiMEM supplemented with 1% penicillin and streptomycin and 5% FBS (Gibco) in an incubator with 5% CO_2 at 37 °C. Primary neuronal cultures were obtained by digestion of mouse cortical tissue dissected at embryo day 17 and were maintained in Neurobasal medium supplemented with B27 and GlutaMax (Gibco). Neuronal culture medium was changed by half volume every 2 to 3 d.

Proximity Ligation Assay (PLA). PLA fluorescence was performed with the Millipore Duolink Kit (54). Briefly, cells on 12-mm coverslips transfected with M1 Aβ42 were fixed in 4% paraformaldehyde for 10 min at RT. After blocking in a heated humidity chamber for 60 min at 37 °C, cells were incubated with two primary antibodies overnight in the cold room and then with PLUS and MINUS PLA probes in a preheated humidity chamber for 1 h at 37 °C. Ligation of two probes with performed at 37 °C for 30 min in a humidity chamber. After several washes, polymerase was added to amplify the signal with Duolink In Situ Detection Reagents green in a preheated humidity chamber for 100 min at 37 °C. Confocal images were taken within 48 h after mounting with Duolink medium with DAPI.

Mitochondrial Isolation, Insoluble Fraction Preparation, and Blue Native PAGE. Cells were harvested by trypsin treatment and washed with room temperature PBS. Resuspended cells were incubated with MSM (220 mM D-mannitol, 70 mM sucrose, and 5 mM MOPS, pH 7.4) on ice for 5 min and homogenized by a 2-mL Dounce homogenizer. Homogenates were centrifuged at 500*g* for 10 min, and the supernatants were further centrifuged for 9,000*g* for 10 min. The obtained pellet was crude mitochondria and was subjected to Percoll gradient centrifugation to obtain purified mitochondria. To prepare insoluble mitochondrial protein aggregates, mitochondria were subjected to 0.1% NP-40 lysis buffer for 30 min on ice and centrifuged at 18,000*g* at 4 °C for half hour, and the pellet was resuspended in Laemmli buffer for SDS-PAGE. For blue native PAGE (55), mitochondrial fractions were lysed by digitonin in native buffer on ice for 20 min and centrifuged at 18,000*g* for 20 min. The supernatants were subjected to blue native electrophoresis by 4–16% Bis-Tris Protein Gels (Invitrogen).

The ATP-dependent Protease Activity Assay of LONP1 In Vitro. C-terminal Myc-tagged LONP1 plasmids were transfected in M17 cells for 72 h, and cells were lysed in RIPA buffer. LONP1-Myc was immune captured by magnetic anti-Myc beads (Thermo, #88842) at room temperature for 1 h. Beads were washed for three times with PBS buffer and then incubated with Myc-peptide in PBS (Thermo, #20170) for 30 min at 37 °C to elute LONP1-Myc proteins. LONP1-Myc

proteins were incubated with FTC-casein (Thermo, #23267) for 30 min at room temperature as described by supplier and the fluorescence read at 485/538 nm for excitation/emission. To analyze ATP-dependent protease activity in isolated mitochondria, mitochondria reconstituted in 1% digitonin lysis buffer were subjected to FTC-casein assay. For ATP-dependent protease activity in intact mitochondria, mouse brain tissues were incubated with or without ATP (10 mM) at room temperature overnight as described previously; then, the ATP-dependent protease cleavage of mitochondrial proteins was analyzed by western blot.

Animal Brain Stereotactic Injection and Behavior Tests. Animals were anesthetized using isoflurane and placed in a stereotactic frame for injection for the dorsal hippocampus, CA1 (AP−2.1 mm, ML−2.0 mm from the bregma) (56). A 10-μL microliter syringe (Hamilton) was filled with virus, and the needle was lowered down 1.4 mm from the bregma. One microliter virus (10^8 viral particles/mL) was injected within 5 min and the needle left in place for another 5 min. Three months after virus injection, animals were subjected to spatial Y-maze test for short-term working memory. The spatial Y-maze test consisted of two trials. The first trial (training) allowed 5-min exploration of the Y maze with one arm (novel arm) blocked, so the mouse only explored two arms (start arm and other arm) of the maze. After an intertrial interval (ITI) of 2 h, the second trial (testing/retention) was conducted. For this trial, the mouse was placed back in the maze in the same starting arm, with free access to all three arms for 5 min. Novelty vs. familiarity was later analyzed from video recordings for the duration, distance, and number of visits in each arm. For fear conditioning test, animals were placed in a conditioning box for a 2-min acclimation period, followed by four rounds of conditional stimulus (tone), and aversive unconditional stimulus (foot shock), followed by another 2 min in the chamber. After an ITI of 24 h, mice are returned to the chamber with no stimulus, and freezing behavior is recorded for 5 min to evaluate context-dependent fear. After behavior tests, the brain was dissected out and immersion fixed in 10% paraformaldehyde for frozen section. All animal experiments followed approved protocols by the Institutional Animal Care and Use Committee (IACUC) of Case Western Reserve University.

Statistical Analysis. All these data were independently assessed and collected by investigators without prior knowledge of samples. Statistical analysis was done with one-way or two-way ANOVA followed by multiple comparison test or Student's *t* test. Data were normally distributed with similar variance between the groups. All statistical analyses were performed blindly to samples information.

Data, Materials, and Software Availability. The proteomic dataset of the mitochondrial Aβ42 interactome was deposited in the figshare database https://figshare.com/ (57). All other data are included in the manuscript and/or *SI Appendix*.

ACKNOWLEDGMENTS. The work was supported in part by the NIH (R01AG076917 and R03AG063362 to W.W. and NS083498, AG049479, and AG083811 to X. Z.), the Clinical and Translational Science Collaborative of Cleveland (UL1TR0002548, pilot award to W. Wang); and Alzheimer's Association (AARG-21-852438 to W.W.). W.W. was a program participant in the Research Education Component of the Cleveland Alzheimer's Disease Research Center supported by NIA P30 AG062428 and AG072959.

Author affiliations: [a]Department of Pathology, Case Western Reserve University, Cleveland, OH 44106; and [b]Electron Microscopy Core Facility, Case Western Reserve University, Cleveland, OH 44106

Author contributions: W.W. and X.Z. designed research; W.W., X.M., S.B., C.S., F.Z., H.F., S.T., and F.W. performed research; W.W., X.M., and X.Z. analyzed data; and W.W. and X.Z. wrote the paper.

1. J. R. Friedman, J. Nunnari, Mitochondrial form and function. *Nature* **505**, 335–343 (2014).
2. L. J. Foster *et al.*, A mammalian organelle map by protein correlation profiling. *Cell* **125**, 187–199 (2006).
3. S. E. Calvo, V. K. Mootha, The mitochondrial proteome and human disease. *Ann. Rev. Genom. Hum. Genet.* **11**, 25–44 (2010).
4. W. Voos, Mitochondrial protein homeostasis: The cooperative roles of chaperones and proteases. *Res. Microbiol.* **160**, 718–725 (2009).
5. W. Voos, Chaperone–protease networks in mitochondrial protein homeostasis. *Biochim. Biophys. Acta* **1833**, 388–399 (2013).
6. S. H. Bernstein *et al.*, The mitochondrial ATP-dependent Lon protease: A novel target in lymphoma death mediated by the synthetic triterpenoid CDDO and its derivatives. *Blood* **119**, 3321–3329 (2012).
7. Y. Ruan *et al.*, Loss of Yme1L perturbates mitochondrial dynamics. *Cell Death Dis.* **4**, e896 (2013).
8. H. Tang *et al.*, Downregulation of HSP60 disrupts mitochondrial proteostasis to promote tumorigenesis and progression in clear cell renal cell carcinoma. *Oncotarget* **7**, 38822–38834 (2016).
9. S. S. Deepa *et al.*, Down-regulation of the mitochondrial matrix peptidase ClpP in muscle cells causes mitochondrial dysfunction and decreases cell proliferation. *Free Radical. Biol. Med.* **91**, 281–292 (2016).
10. H. Unal Gulsuner *et al.*, Mitochondrial serine protease HTRA2 p.G399S in a kindred with essential tremor and Parkinson disease. *Proc. Natl. Acad. Sci. U.S.A.* **111**, 18285–18290 (2014).
11. E. M. Jenkinson *et al.*, Perrault syndrome is caused by recessive mutations in CLPP, encoding a mitochondrial ATP-dependent chambered protease. *Am. J. Hum. Genet.* **92**, 605–613 (2013).
12. K. A. Strauss *et al.*, CODAS syndrome is associated with mutations of LONP1, encoding mitochondrial AAA+ Lon protease. *Am. J. Hum. Genet.* **96**, 121–135 (2015).
13. P. Martinelli, E. I. Rugarli, Emerging roles of mitochondrial proteases in neurodegeneration. *Biochim. Biophys. Acta* **1797**, 1–10 (2010).
14. B. Hartmann *et al.*, Homozygous YME1L1 mutation causes mitochondriopathy with optic atrophy and mitochondrial network fragmentation. *eLife* **5**, e16078 (2016).
15. H.-G. Goo, M. K. Jung, S. S. Han, H. Rhim, S. Kang, HtrA2/Omi deficiency causes damage and mutation of mitochondrial DNA. *Biochim. Biophy. Acta (BBA): Mol. Cell Res.* **1833**, 1866–1875 (2013).
16. W. Wang, F. Zhao, X. Ma, G. Perry, X. Zhu, Mitochondria dysfunction in the pathogenesis of Alzheimer's disease: Recent advances. *Mol. Neurodegener.* **15**, 30 (2020).
17. H. M. Wilkins, R. H. Swerdlow, Mitochondrial links between brain aging and Alzheimer's disease. *Transl. Neurodegener.* **10**, 33 (2021).
18. K. Hirai *et al.*, Mitochondrial abnormalities in Alzheimer's disease. *J. Neurosci.* **21**, 3017–3023 (2001).
19. P. H. Reddy *et al.*, Mutant APP and amyloid beta-induced defective autophagy, mitophagy, mitochondrial structural and functional changes and synaptic damage in hippocampal neurons from Alzheimer's disease. *Hum. Mol. Genet.* **27**, 2502–2516 (2018).
20. E. Trushina *et al.*, Defects in mitochondrial dynamics and metabolomic signatures of evolving energetic stress in mouse models of familial Alzheimer's disease. *PLoS ONE* **7**, e32737 (2012).
21. D. F. Silva *et al.*, Bioenergetic flux, mitochondrial mass and mitochondrial morphology dynamics in AD and MCI cybrid cell lines. *Hum. Mol. Genet.* **22**, 3931–3946 (2013).
22. S. Han, M. Zhang, Y. Y. Jeong, D. J. Margolis, Q. Cai, The role of mitophagy in the regulation of mitochondrial energetic status in neurons. *Autophagy* **17**, 4182–4201 (2021).
23. X. Wang *et al.*, Impaired balance of mitochondrial fission and fusion in Alzheimer's disease. *J. Neurosci.* **29**, 9090–9103 (2009).
24. S. J. Beck *et al.*, Deregulation of mitochondrial F1FO-ATP synthase via OSCP in Alzheimer's disease. *Nat. Commun.* **7**, 11483 (2016).
25. J. W. Lustbader *et al.*, ABAD directly links Abeta to mitochondrial toxicity in Alzheimer's disease. *Science* **304**, 448–452 (2004).
26. C. A. Hansson Petersen *et al.*, The amyloid beta-peptide is imported into mitochondria via the TOM import machinery and localized to mitochondrial cristae. *Proc. Natl. Acad. Sci. U.S.A.* **105**, 13145–13150 (2008).
27. M. Manczak *et al.*, Mitochondria are a direct site of A beta accumulation in Alzheimer's disease neurons: Implications for free radical generation and oxidative damage in disease progression. *Hum. Mol. Genet.* **15**, 1437–1449 (2006).
28. D. Mossmann *et al.*, Amyloid-beta peptide induces mitochondrial dysfunction by inhibition of preprotein maturation. *Cell Metabol.* **20**, 662–669 (2014).
29. H. Du *et al.*, Cyclophilin D deficiency attenuates mitochondrial and neuronal perturbation and ameliorates learning and memory in Alzheimer's disease. *Nat. Med.* **14**, 1097–1105 (2008).
30. G. Perry, A. D. Cash, M. A. Smith, Alzheimer disease and oxidative stress. *J. Biomed. Biotechnol.* **2**, 120–123 (2002).
31. Q. Cai, P. Tammineni, Alterations in mitochondrial quality control in Alzheimer's disease. *Front. Cell Neurosci.* **10**, 24 (2016).
32. R. Sultana, D. A. Butterfield, Oxidatively modified, mitochondria-relevant brain proteins in subjects with Alzheimer disease and mild cognitive impairment. *J. Bioenerg. Biomembr.* **41**, 441–446 (2009).
33. M. P. Murphy, H. LeVine IIIrd., Alzheimer's disease and the amyloid-beta peptide. *J. Alzheimers Dis.* **19**, 311–323 (2010).
34. A. Smilansky *et al.*, The voltage-dependent anion channel 1 mediates amyloid β toxicity and represents a potential target for Alzheimer disease therapy. *J. Biol. Chem.* **290**, 30670–30683 (2015).
35. K. D. Meyer *et al.*, Comprehensive analysis of mRNA methylation reveals enrichment in 3' UTRs and near stop codons. *Cell* **149**, 1635–1646 (2012).
36. F. Zhao *et al.*, METTL3-dependent RNA m(6)A dysregulation contributes to neurodegeneration in Alzheimer's disease through aberrant cell cycle events. *Mol. Neurodegener.* **16**, 70 (2021).
37. E. F. Vieux, M. L. Wohlever, J. Z. Chen, R. T. Sauer, T. A. Baker, Distinct quaternary structures of the AAA+ Lon protease control substrate degradation *Proc. Natl. Acad. Sci. U.S.A.* **110**, E2002–E2008 (2013).
38. W. Wang *et al.*, Inhibition of mitochondrial fragmentation protects against Alzheimer's disease in rodent model. *Hum. Mol. Genet.* **26**, 4118–4131 (2017).
39. T. G. Demarest *et al.*, Sex dependent alterations in mitochondrial electron transport chain proteins following neonatal rat cerebral hypoxic-ischemia. *J. Bioenerg. Biomembr.* **48**, 591–598 (2016).
40. T. G. Demarest *et al.*, Sex-dependent mitophagy and neuronal death following rat neonatal hypoxia-ischemia. *Neuroscience* **335**, 103–113 (2016).
41. T. G. Demarest, R. A. Schuh, J. Waddell, M. C. McKenna, G. Fiskum, Sex-dependent mitochondrial respiratory impairment and oxidative stress in a rat model of neonatal hypoxic-ischemic encephalopathy. *J. Neurochem.* **137**, 714–729 (2016).
42. J. S. Kerr *et al.*, Mitophagy and Alzheimer's disease: Cellular and molecular mechanisms. *Trends Neurosci.* **40**, 151–166 (2017).
43. E. F. Fang *et al.*, Mitophagy inhibits amyloid-β and tau pathology and reverses cognitive deficits in models of Alzheimer's disease. *Nat. Neurosci.* **22**, 401–412 (2019).
44. A. Fleming *et al.*, The different autophagy degradation pathways and neurodegeneration. *Neuron* **110**, 935–966 (2022).

45. F. Muñoz-Carvajal, M. Sanhueza, The mitochondrial unfolded protein response: A hinge between healthy and pathological aging. *Front. Aging Neurosci.* **12**, 581849 (2020).
46. J. S. Beck, E. J. Mufson, S. E. Counts, Evidence for mitochondrial UPR gene activation in familial and sporadic Alzheimer's disease. *Curr. Alzheimer Res.* **13**, 610–614 (2016).
47. V. Sorrentino *et al.*, Enhancing mitochondrial proteostasis reduces amyloid-beta proteotoxicity. *Nature* **552**, 187–193 (2017).
48. S. Pickles, P. Vigie, R. J. Youle, Mitophagy and quality control mechanisms in mitochondrial maintenance. *Curr. Biol. CB* **28**, R170–R185 (2018).
49. S. G. Kang, M. N. Dimitrova, J. Ortega, A. Ginsburg, M. R. Maurizi, Human mitochondrial ClpP is a stable heptamer that assembles into a tetradecamer in the presence of ClpX. *J. Biol. Chem.* **280**, 35424–35432 (2005).
50. N. Hoogenraad, A brief history of the discovery of the mitochondrial unfolded protein response in mammalian cells. *J. Bioenerg. Biomembr.* **49**, 293–295 (2017).
51. Y. Shen *et al.*, Activation of mitochondrial unfolded protein response in SHSY5Y expressing APP cells and APP/PS1 mice. *Front. Cell Neurosci.* **13**, 568 (2019).
52. D. Sirk *et al.*, Chronic exposure to sub-lethal beta-amyloid (Abeta) inhibits the import of nuclear-encoded proteins to mitochondria in differentiated PC12 cells. *J. Neurochem.* **103**, 1989–2003 (2007).
53. A. Hoshino *et al.*, Oxidative post-translational modifications develop LONP1 dysfunction in pressure overload heart failure. *Circ. Heart Fail.* **7**, 500–509 (2014).
54. Y. Liu *et al.*, DJ-1 regulates the integrity and function of ER-mitochondria association through interaction with IP3R3-Grp75-VDAC1. *Proc. Natl. Acad. Sci. U.S.A.* **116**, 25322–25328 (2019).
55. L. Zhou, W. Wang, C. Hoppel, J. Liu, X. Zhu, Parkinson's disease-associated pathogenic VPS35 mutation causes complex I deficits. *Biochim. Biophys. Acta: Mol. Basis Dis.* **1863**, 2791–2795 (2017).
56. W. Wang *et al.*, Parkinson's disease-associated mutant VPS35 causes mitochondrial dysfunction by recycling DLP1 complexes. *Nat. Med.* **22**, 54–63 (2016).
57. W. Wang, The interactome of mitochondrial aβ-42 in M17 cells. Figshare data repository. https://doi.org/10.6084/m9.figshare.24262984.v1. Deposited 30 October 2023.